

# Correlations of Structure and Dynamics in an Aging Colloidal Glass

Gianguido C. Cianci, Rachel E. Courtland and Eric R. Weeks \*

*Department of Physics, Emory University, Atlanta, GA 30322, U.S.A.*

---

## Abstract

We study concentrated colloidal suspensions, a model system which has a glass transition. Samples in the glassy state show aging, in that the motion of the colloidal particles slows as the sample ages from an initial state. We study the relationship between the static structure and the slowing dynamics, using confocal microscopy to follow the three-dimensional motion of the particles. The structure is quantified by considering tetrahedra formed by quadruplets of neighboring particles. We find that while the sample clearly slows down during aging, the static properties as measured by tetrahedral quantities do not vary. However, a weak correlation between tetrahedron shape and mobility is observed, suggesting that the structure facilitates the motion responsible for the sample aging.

*Key words:* A. Disordered systems, D. Order-disorder effects, D. Phase transitions.  
*PACS:* 05.70.Ln, 61.43.Fs, 64.70.Pf, 82.70.Dd

---

## 1 Introduction

When some liquids undergo a rapid temperature quench they can form glasses. This occurs at a glass transition temperature  $T_g$  which often depends on the cooling rate. As the system is cooled, the approaching glass transition is marked by a dramatic increase in the macroscopic viscosity of the liquid, and a corresponding increase in the microscopic time scales for motion [1–4]. Both the viscosity and the microscopic relaxation time can change by many orders of magnitude as the temperature decreases by merely 10%. Once in the glass state, another phenomenon is noted, that of aging: the dependence of the properties of the system on the time elapsed since reaching  $T_g$ . When such behavior is observed the system is said to be out of equilibrium, a fact that

---

\* For correspondence: weeks@physics.emory.edu

could be anticipated by noting that the dependence of  $T_g$  itself on cooling rate implies the glass transition is not an equilibrium phenomenon. Aging most prominently manifests itself in the dynamics: the microscopic relaxation time scale depends on the age of the sample.

Attempts to explain these phenomena try to link the microscopic structure to the microscopic dynamics. For example, one might postulate that the increase in viscosity is caused by the growth of domains whose dynamics are correlated [5]. However, no experiment has seen a structural length scale characterizing such domains that grows or diverges at  $T_g$  [1,6,7]. Likewise, aging might be due to some coarsening of structure; as domains of glassy structure grow, motion is slowed, which in turn slows the further growth of these domains. However, these domains have not been identified, and currently no structural features have been identified that explain aging dynamics [8,9].

Recently, some interesting developments in the study of aging non-equilibrium systems have been brought about by the adoption of dense colloidal suspensions as model systems for liquids, glasses and gels [7,8,10–13]. Colloidal suspensions consist of solid particles in a liquid, and the motion of the particles is analogous to that of atoms or molecules in a more traditional material [10,14,15]. In these systems, the particle interactions can easily be tuned from repulsive to attractive. A common case is when particles interact simply as hard spheres with no interactions, attractive or repulsive, other than when they are in direct contact [10,16]. In all cases, a major control parameter is the packing fraction  $\phi$ . For hard spheres this is the only control parameter and when  $\phi$  is raised above a value of  $\phi_g \approx 0.58$  the system becomes glassy and the aging process begins.

While structural changes in an aging system remain unclear, two experiments studying colloids have characterized the dynamics. Cipelletti and co-workers [12] studied aging in a colloidal gel using novel light scattering techniques and showed that the dynamics in such a non-equilibrium system present striking temporal heterogeneities. Aging has also been studied in a colloidal glass using confocal microscopy [13]. In that study both temporal and spatial heterogeneities were seen. However, despite the ease with which a colloidal glass can be formed and observed a detailed understanding of the structural changes that accompany aging and the slowing of dynamics has not yet been seen.

In this paper we study the structure of an aging colloidal glass by considering how colloids pack together. Entropy can be maximized by optimizing packing in a dense suspension. Consider the intriguing case of the crystallization of hard spheres. When spheres arrange into a crystalline lattice, they lose configurational entropy. However, they each have more local room to move close to their lattice site, and thus the vibrational entropy is larger. This increase in vibrational entropy outweighs the loss of configurational entropy due to

crystallization [17]. In practice, this argument holds true for systems with volume fractions above  $\phi_{\text{freeze}} = 0.494$ , the point at which the system begins to nucleate crystals; below  $\phi_{\text{freeze}}$ , the configurational entropy dominates and the system prefers an amorphous, liquid configuration [10].

For glasses, we consider a different sort of packing. The most efficient way to pack four spheres of diameter  $d$  in three dimensions is to place them at the vertices of a regular tetrahedron with edge length  $d$ . In this configuration, the effective volume fraction for the four spheres reaches a surprising 0.78. In other words, for a given volume fraction  $\phi$ , locally four particles can maximize their entropy by arranging into a regular tetrahedron consistent with the global volume fraction  $\phi$ , thus giving them additional room to move. However, regular tetrahedra do not tile 3D space and therefore the most efficient macroscopic packing is that of a hexagonally packed crystal at  $\phi_{\text{hcp}} \approx 0.74$ . Thus in a glass there is a *frustration* between the drive to locally pack in tetrahedra to maximize the local volume available to vibrations, and the inability to tile 3D space with such structures. This has been suggested as a possible origin for the glass transition in simple liquids [18–21].

We take advantage of the insight afforded to us by fast laser scanning confocal microscopy [7,14,15,22] and study an aging colloidal glass in terms of tetrahedral packing. We focus on geometrical properties of the tetrahedra formed by the colloids and look for correlations between these *static* quantities and the conspicuous slowing of the *dynamics* as measure by the average tetrahedral mobility. We find that while the distribution of these static quantities does not age, they correlate weakly with mobility, suggesting that the structure facilitates the aging process.

## 2 Experimental Methods

We suspend poly(methyl methacrylate) (PMMA) colloids of diameter  $d = 2.36\mu\text{m}$  in a mixture of 15% decalin and 85% cyclohexylbromide by weight. The mixture closely matches the density and refractive index of the particles, thus greatly reducing sedimentation and scattering effects. The size polydispersity of the colloids ( $\approx 5\%$ ) prevents crystallization. The particles are sterically stabilized against van der Waals attractions by a thin layer of poly-12-hydroxystearic acid [23]. We dye the colloids with rhodamine 6G [22]. The particles also carry a slight charge due to the dye. In this paper, we measure all lengths in terms of the diameter  $d$  and all times in terms of  $\tau_{\text{diff}}$ , the time a particle would take to diffuse its own diameter in the *dilute* limit. Given the solvent viscosity  $\eta = 2.25 \text{ mPa}\cdot\text{s}$  at  $T = 295 \text{ K}$ , this time is  $\frac{d^2}{6D} = 11.4 \text{ s}$  where  $D = \frac{k_{\text{B}}T}{3\pi\eta d}$ .

We acquire three dimensional images by fast laser scanning confocal microscopy at a rate of 1 every 26 s. The observation volume measures  $26d \times 25d \times 4.2d$ . At these high densities ( $\phi > 0.58$ ) the colloids move slowly and can easily be tracked using established analysis techniques [15,22,24]. The 3D positions of  $\sim 2500$  particles are measured virtually instantaneously with an accuracy of  $0.013d$  in the  $x - y$  plane and  $0.021d$  along the optical axis. We acquire data at least  $25d$  away from the closest wall, to avoid boundary effects [25,26]. We do not observe any crystals in the bulk even after several weeks.

The phase behavior of this quasi-hard sphere system is controlled by varying the packing fraction  $\phi$ . The system undergoes a glass transition when  $\phi > \phi_g \approx 0.58$  in agreement with what is seen in hard sphere systems [10,15]. Here we present data from a sample at  $\phi \approx 0.62$  though we see qualitatively similar results for all  $\phi > \phi_g$ .

Proper sample initialization is paramount when studying aging and is ensured here by a vigorous, macroscopic stirring. This shear melting effectively rejuvenates the glass and yields reproducible dynamics that depend exclusively on  $t_w$ , the time elapsed since initialization. Data acquisition starts immediately after rejuvenation. Transient macroscopic flows are observable for the first 25 min  $\approx 140\tau_{\text{diff}}$  and we set  $t_w = 0$ , or age zero, when they subside. The results below are insensitive to small variations in this choice.

### 3 Results

We observe our sample for  $\sim 700\tau_{\text{diff}}$  without disturbing it. We then split the data in three time windows as follows:  $[0 - 100\tau_{\text{diff}}]$ ,  $[100 - 300\tau_{\text{diff}}]$  and  $[300 - 700\tau_{\text{diff}}]$ . This corresponds to doing three experiments with samples aged  $t_w = 0, 100$  and  $300\tau_{\text{diff}}$  respectively. The dynamics slow as the sample ages, as shown in Fig. 1, where we plot the mean square displacement for the three data portions averaged over all particles and over all initial times within a given time window. At short and medium times ( $\frac{\Delta t}{\tau_{\text{diff}}} < 10$ ), particle motions are subdiffusive as indicated by a slope less than unity on the log-log plot. At longer times the slope tends to one; the time scale for this upturn changes dramatically for different values of age  $t_w$  clearly indicating that the sample is out of equilibrium. It is this slowing down of dynamics that we wish to analyze in terms of tetrahedral structure.

We start our structural analysis by calculating the pair correlation function  $g(r)$  and plot the result in Fig. 2. This function does not vary with age and thus is calculated by averaging over all times. The first peak of  $g(r)$  is at  $r = 1.04d$  which deviates somewhat from the ideal hard-sphere position ( $r = d$ ). This can be explained by the slight charging mentioned above and perhaps also by

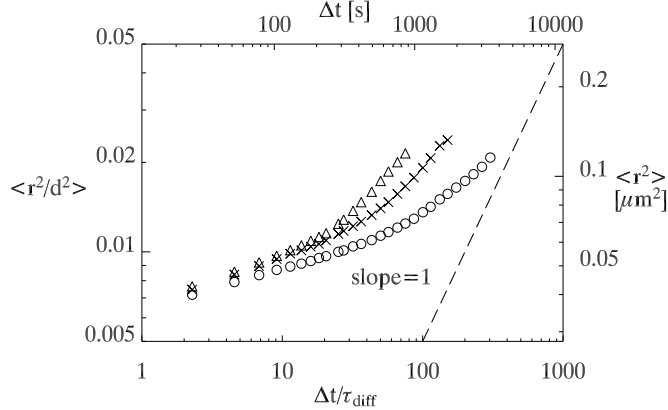


Fig. 1. Aging mean squared displacement for a colloidal glass at  $\phi \approx 0.62$ . The three curves represent three different ages of the sample.  $\triangle$  :  $t_w = 0\tau_{\text{diff}}$ ,  $\times$  :  $t_w = 100\tau_{\text{diff}}$  and  $\circ$  :  $t_w = 300\tau_{\text{diff}}$ . The dashed line has a slope of 1 and represents diffusive behavior, not seen in this glassy sample.

the uncertainty in the value of the particle diameter which we deem to be at most 2%. Figure 2 also shows the characteristic double second peak found in many glassy systems.

In order to study the tetrahedral packing in our sample we begin by labeling as nearest neighbors every pair of colloids whose separation is within the first peak of  $g(r)$ , namely  $0.74d > r > 1.38d$ , as is shown by the shaded area in Fig. 2. The lower limit is chosen to eliminate artificially close pairs which arise from the occasional error in particle identification, while the upper limit corresponds to the first minimum of  $g(r)$ . Note that a completely coplanar arrangement of four spheres in a square is excluded as a tetrahedron, as the diagonal would have length  $\sqrt{2}d$  which is excluded by our upper limit. The results presented here are insensitive to small variations in these parameters and match those obtained using Delaunay triangulation as a nearest neighbor finding algorithm.

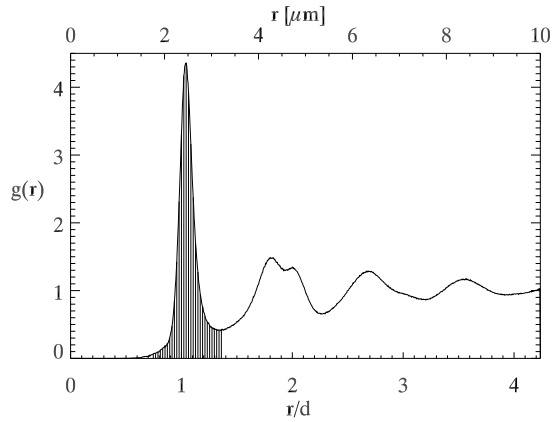


Fig. 2. Pair correlation function  $g(r)$ . The shaded area indicates the range of inter-particle distances used to define nearest neighbors.

A tetrahedron is then defined as a quadruplet of mutually nearest neighbor colloids. To characterize each tetrahedron, we calculate several geometrical characteristics. The first is “looseness”  $b$ , defined as the average of the lengths of the 6 edges, or “bond lengths”,  $b_i$ . An “irregularity”  $\sigma_b$  is defined as the standard deviation of the  $b_i$ . The looseness and irregularity appear to be the most important geometric parameters to characterize a tetrahedron shape, as will be discussed below. The nondimensional tetrahedral volume  $V/d^3$  and surface area  $A/d^2$  are also measured using the usual expressions:

$$V = \frac{1}{3!} |\mathbf{b}_{ij} \cdot (\mathbf{b}_{ik} \times \mathbf{b}_{il})| \quad (1)$$

$$A = \frac{1}{2} (|\mathbf{b}_{ij} \times \mathbf{b}_{ik}| + |\mathbf{b}_{ij} \times \mathbf{b}_{il}| + |\mathbf{b}_{ik} \times \mathbf{b}_{il}| + |\mathbf{b}_{jk} \times \mathbf{b}_{il}|) \quad (2)$$

where  $\mathbf{b}_{mn}$  is the vector from vertex (particle)  $m$  to vertex  $n$ .

To quantify an effective aspect ratio of each tetrahedron, we calculate the height of the tetrahedron as measured from each of the four faces, and consider the largest height  $H$  and shortest height  $h$ . We form aspect ratios from these two heights by dividing by the areas ( $A_H$  and  $A_h$  respectively) of the tetrahedron face they are perpendicular to. Conceptually, large values of  $H^2/A_H$  correspond to thin pointy tetrahedra, and small values of  $h^2/A_h$  correspond to flat pancake-like tetrahedra. We thus term these two quantities “sharpness” and “flatness” respectively.

In addition to these structural characteristics, we also consider the dynamics by the tetrahedral mobility  $\mu$ , which is calculated by averaging the distances moved by the four colloids over a time  $\Delta t = 50\tau_{\text{diff}}$ :

$$\mu(t) = \frac{1}{4} \sum_{i=1}^4 |\Delta \vec{r}_i(t, \Delta t)| = \langle |\Delta \vec{r}_i(t, \Delta t)| \rangle_i \quad (3)$$

The results that follow do not depend sensitively to the choice of  $\Delta t$ . While the four particles must form a tetrahedron at time  $t$ , we only require them to be within the observation volume at time  $t + \Delta t$ , rather than still being mutual nearest neighbors.

To assess the value of these structural and dynamical characteristics, we calculate the correlation coefficients between  $\mu$  and the other tetrahedral characteristics and show them in Table 1. This is done in the standard way of defining correlation coefficients,

$$C_{pq} = \frac{1}{N} \sum_{i=1}^N \frac{(p_i - \bar{p})}{\sigma_p} \frac{(q_i - \bar{q})}{\sigma_q}, \quad (4)$$

	$\mu/d$	$b/d$	$\sigma_b/d$	$V/d^3$	$A/d^2$	$\frac{H^2}{A_H}$	$\frac{h^2}{A_h}$
mobility $\mu/d$	1	0.045	0.07	0.018	0.036	0.016	-0.07
“looseness” $b/d$	-	1	0.37	0.82	0.98	-0.30	-0.50
“irregularity” $\sigma_b/d$	-	-	1	-0.10	0.18	0.17	-0.82
volume $V/d^3$	-	-	-	1	0.91	-0.10	-0.11
surface area $A/d^2$	-	-	-	-	1	-0.29	-0.37
“sharpness” $\frac{H^2}{A_H}$	-	-	-	-	-	1	-0.091
“flatness” $\frac{h^2}{A_h}$	-	-	-	-	-	-	1

Table 1

Correlation matrix for some geometrical characteristics of tetrahedra and mobility. The matrix is symmetric with respect to the diagonal so the lower half is not repeated.  $b$  is the average length of the tetrahedra edges (“bonds”) and  $\sigma_b$  is the standard deviation of these lengths. See text for details of the other characteristics. The coefficients reported with three significant digits have an uncertainty of 0.005, those reported with two significant figures have an uncertainty of 0.01

where  $p$  and  $q$  are any two variables with averages  $\bar{p}$  and  $\bar{q}$ , and standard deviations  $\sigma_p$  and  $\sigma_q$ . In our case the sum runs over all tetrahedra and all times. Equation 4 can be generalized to measure  $C_{p(t)q(t+\tau)}$ , the correlation between variable  $p$  at time  $t$  and variable  $q$  at a later time  $t+\tau$ . Both  $C_{\mu(t)b(t+\tau)}$  and  $C_{\mu(t)\sigma_b(t+\tau)}$  show an increase for  $\tau < \Delta t$ , but this has a simple explanation: more mobile tetrahedra tend to expand (increasing  $b$  and  $\sigma$  on average) and thus  $\mu(t)$  is correlated with  $b(t+\tau)$  and  $\sigma(t+\tau)$ . For all other pairs of variables, we observe a smooth monotonic decorrelation as function of lag time. We therefore focus our attention on the simpler case of  $\tau = 0$ . In Table 1, a value of one would signify perfect correlation, a value of -1 would represent perfect anti-correlation while a value of zero would indicate completely uncorrelated data.

We also analyzed the mobility of the center of mass of the tetrahedra, or “translation”,  $\mu_c(t) = |\langle \Delta \vec{r}_i \rangle_i|$ , and the “expansion” with respect to the center of mass,  $\mu_e(t) = \langle |\Delta \vec{r}_i - \langle \Delta \vec{r}_i \rangle_i| \rangle_i$  (data not shown). We found  $C_{\mu_c q}$  to be zero for all static quantities  $q$  (within our uncertainties). This signifies that the translation of the tetrahedra is independent of the geometrical characteristics. On the other hand, we found  $C_{\mu_e q}$  to be slightly larger than the corresponding  $C_{\mu q}$ . This indicates that statics instead do influence the expansion of tetrahedra. In some sense  $\mu$  is a combination of  $\mu_c$  and  $\mu_e$  and by calculating the latter two quantities we highlight the fact that not all types of mobilities are equivalent when studied in relation to statics. In particular, expansion is the dynamical quantity most sensitive to changes in structure as measured by tetrahedra. However, here we choose to present our results in terms of  $\mu$  because it is a simpler quantity and maintains the same qualitative behavior.

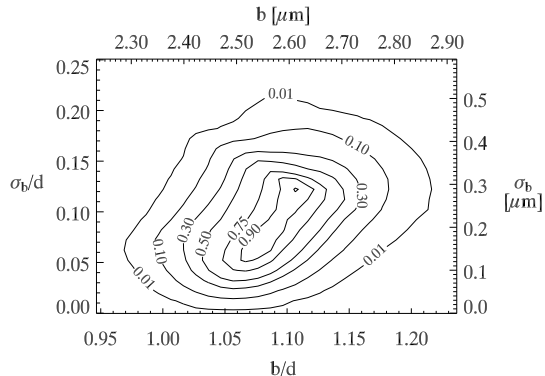


Fig. 3. Contour plot showing the abundance of tetrahedra with a given looseness and irregularity. The iso-curves are labeled relative to the peak tetrahedral abundance at  $\{b/d = 1.11; \sigma_b/d = 0.12\}$ .

Given that we are trying to understand the slowing of the dynamics seen in Fig. 1, we focus on the correlation between mobility  $\mu/d$  and the structural characteristics. While all the coefficients are quite small, those that relate mobility to looseness  $b/d$  and irregularity  $\sigma_b/d$  are relatively big. Mobility is also noticeably anticorrelated with the flatness  $h^2/A_h$ . Some insight into these correlations is gained by considering the correlations between the different structural characteristics, as shown by the other entries in Table 1. The flatness  $h^2/A_h$  is strongly anticorrelated with irregularity  $\sigma_b$ , and given the more intuitive nature of  $\sigma_b$  and its simpler mathematical definition, in what follows we focus on  $\sigma_b$  rather than  $h^2/A_h$ . The volume and area parameters,  $V/d^3$  and  $A/d^2$ , are strongly correlated with the looseness, which is sensible given that they all measure the size of a tetrahedron.

We therefore choose to study the looseness and irregularity as being both relatively well-correlated with mobility, both easily defined in terms of the six tetrahedron edge lengths, and weakly correlated with each other (as seen in Table 1). The last point suggests that they capture two distinct properties of tetrahedron structure which are both important for mobility.

Figure 3 shows the distribution of tetrahedra in the  $b, \sigma_b$ -plane. The closed curves represent the levels of abundance of tetrahedra with a given value of  $b$  and  $\sigma_b$  with respect to the abundance of the most probable tetrahedron at  $b \approx 1.11d$  and  $\sigma_b \approx 0.12d$ . Somewhat surprisingly, the distribution does not age [27] and we therefore take an average over all times. Figure 3 shows a broad variability of both looseness and irregularity. However, these curves do outline a major axis along which many of the tetrahedra lie. This axis suggests that the looser the tetrahedron the more irregular it is bound to be. This is reflected in the correlation coefficient of  $b$  and  $\sigma_b$  in Table 1, although its relatively small value (0.37) highlights the breadth of the overall distribution.

We present a qualitative picture of the relationship between the above two



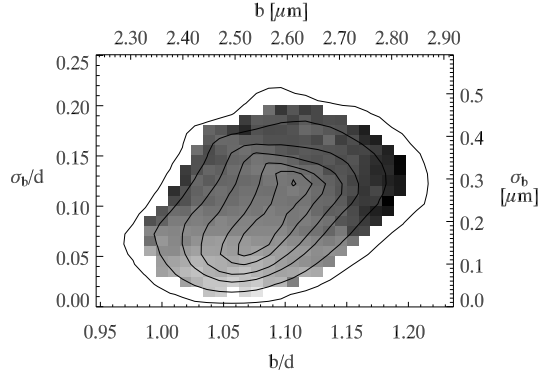


Fig. 4. Plot of tetrahedral mobility  $\langle \mu(\Delta t = 50\tau_{\text{diff}}) \rangle$ , averaged over all ages, versus looseness  $b/d$  and irregularity  $\sigma_b/d$ . The darker the color the more mobile the tetrahedron. The contour lines are the same as in Fig. 3 and represent the abundance of tetrahedra with a given value of  $b/d$  and  $\sigma_b/d$ .

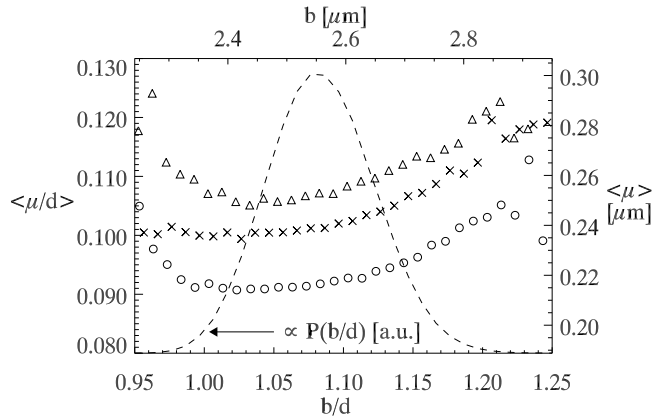


Fig. 5. Average tetrahedral mobility as a function of looseness  $b/d$ . The three curves represent three different ages of the sample.  $\triangle$  :  $t_w = 0\tau_{\text{diff}}$ ,  $\times$  :  $t_w = 100\tau_{\text{diff}}$  and  $\circ$  :  $t_w = 300\tau_{\text{diff}}$ . The dashed curve represents the distribution  $P(b/d)$  and is shown here to highlight the lack of statistics at low ( $b/d < 0.98$ ) and high ( $b/d > 1.2$ ) values of  $b/d$ .

*static* geometrical quantities and the *dynamic* quantity of mobility in Fig. 4 which shows the average value of mobility as a shade of grey. The more mobile combinations of  $b$  and  $\sigma_b$  are darker and the less mobile combinations are lighter. This rendering gives a clear qualitative view of the correlations between these quantities. Specifically, we note that mobility increases with both looseness and irregularity of the tetrahedron. This makes intuitive sense: a larger value of  $b$  suggests a smaller local volume fraction and thus more room to move, and a larger value of  $\sigma_b$  likewise suggests a poorly-packed structure which may have more room to move. This also agrees with previous results seen in supercooled colloidal fluids [28–30]. Overplotted on the intensity plot of Fig. 4 are the same abundance contours as seen in Fig. 3, showing us that the most probable tetrahedra are a medium shade of grey - they are neither the fastest or slowest tetrahedra.

We thus have two results, an overall slowing of dynamics seen in Fig. 1, and a relationship between structure and dynamics seen in Fig. 4. This suggests a possible hypothesis for aging, that the slowing of the dynamics is an accumulation of structure corresponding to slower dynamics: a buildup of tetrahedra with small values for looseness and irregularity. As mentioned earlier, though, the overall distribution of tetrahedra structural properties (Fig. 3) does not depend on the age of the sample [27]. To reconcile this, we consider in more detail the connection between structure, dynamics, and the age of the sample.

We show the influence of looseness on the tetrahedron mobility in Fig. 5 where we plot the average mobility of tetrahedra as a function of looseness. We do so averaging over the three sample ages separately. If we consider each curve separately, we note a reproducible trend: the least mobile tetrahedra are those with  $b \approx d$  indicating that those tetrahedra are very tightly packed. At very low values of  $b$  mobility increases somewhat, although as mentioned above, tetrahedra with  $b/d < 1$  may be erroneous. Furthermore, note that there are extremely few tetrahedra with  $b/d < 1$  as shown by the dashed curve representing  $P(b/d)$ , the probability of finding a tetrahedron with a given looseness averaged over all ages. We therefore cannot put too much weight on the values of  $\mu$  for  $b < d$ . (The same can be said for tetrahedra with  $b > 1.17d$ .) In the intermediate range there is a clear trend that looser tetrahedra are more mobile. Thus the structure in some way facilitates the aging, in that looser regions are more free to rearrange. However, it is also important to note that each symbol is an average over a broad distribution of mobilities associated with the given value of  $b/d$ . In particular the standard deviation of the distribution is almost comparable with the average value. This simply means that the correlation between  $b$  and  $\mu$  is a weak, average effect and not, for example, a usefully predictive relationship [30].

As expected with any plot involving the mobility of this system, aging is clearly visible in Fig. 5 as the three curves are shifted down to lower mobilities as  $t_w$  increases. The overall shape of the curves, however, does not depend on the age of the system. In other words, we are not witnessing a relative shift in the mobility of tetrahedra with varying looseness but merely an overall slowing down of all tetrahedra.

A similar analysis on the relation between tetrahedral mobility and irregularity is shown on Fig. 6. As a reference we plot  $P(\sigma_b/d)$ , the probability of finding a tetrahedron with a given irregularity. This distribution does not age and is therefore averaged over all times. Again, we look at the dependence of  $\mu$  on  $\sigma_b$  for the three ages in our experiments and find that there is a positive correlation, as previously indicated in Table 1. Just as in the case of  $b$ , this positive correlation is an average effect and again, the distribution that leads to each of the symbols on the figure is quite broad. Nevertheless, a reproducible difference of  $\sim 10\%$  in the mobility differentiates very regular tetrahedra from

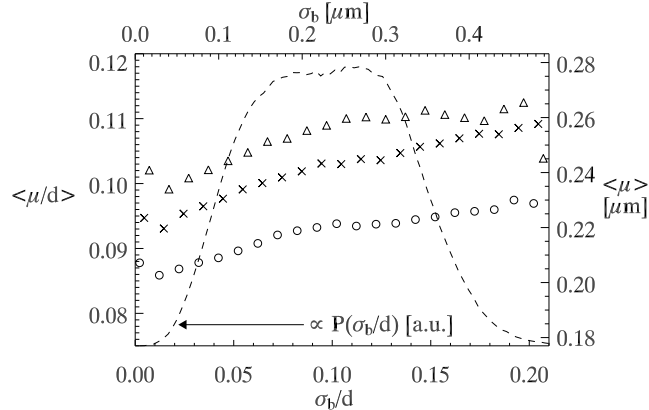


Fig. 6. Average tetrahedral mobility as a function of irregularity  $\sigma_b/d$ . The three curves represent three different ages of the sample.  $\triangle$  :  $t_w = 0\tau_{\text{diff}}$ ,  $\times$  :  $t_w = 100\tau_{\text{diff}}$  and  $\circ$  :  $t_w = 300\tau_{\text{diff}}$ . The dashed curve represents the distribution  $P(\sigma_b/d)$  and is shown here to highlight the lack of statistics at low ( $\sigma_b/d < 0.01$ ) and high ( $\sigma_b/d > 0.2$ ) values of  $\sigma_b/d$ .

very irregular ones. Again, just as above, aging is evident in the data and again it has no strong effect on the shape of the curves but rather uniformly slows down tetrahedra with all values of irregularity.

#### 4 Conclusion

We observe colloidal glasses and find clear signs of aging in the mean squared displacement of the particles (Fig. 1). We analyze the static structure of the aging sample in terms of tetrahedral packing of colloidal particles. We find a broad distribution of tetrahedra sizes and shapes as measured by the distributions of tetrahedral “looseness” and “irregularity”, corresponding to the tetrahedron’s mean edge length and the standard deviation of edge lengths, respectively (Fig. 3). These two quantities are slightly correlated; on average, the looser a tetrahedron is the more irregular it will be. More importantly, we find that tetrahedral shape and mobility are somewhat correlated: the looser and the more irregular a tetrahedron is the higher its mobility (Fig. 4). This suggests that aging might be due to an increase in tight, regular tetrahedral structure, but surprisingly the distribution of geometrical quantities is age-independent. Instead we find that aging indiscriminately affects tetrahedra with all values of looseness and irregularity by uniformly decreasing their mobility.

In conclusion, we find that static structure as measured by tetrahedral quantities does not indicate the age of a glass. None of the distributions of the geometrical quantities considered in Table 1 show any aging. However, at any instant in time the age of our sample must somehow be encoded in the

positions of the colloids and, for example, analyzing the spatial correlations between tetrahedra, while beyond the scope of this paper, might provide more insight into this matter. Finally, since aging ought to result in subtle configuration changes, and since the looser and more irregular tetrahedra allow for the most motion to happen, we can infer that the local structure does indeed facilitate the aging process. While it is worth noting that it is not established that the most mobile particles are the most important ones for aging, the connection between structure and mobility holds true for less mobile particles as well. Table 1 suggests that in this respect, tetrahedral irregularity is the most significant quantity whose positive correlation with mobility lends support to our original motivating idea that perfect tetrahedra are an important structural element in a glass.

## Acknowledgements

We thank T. Brzinski, P. Harrowell, and C. Nugent for useful discussions. This work was supported by NASA microgravity fluid physics grant NAG3-2728.

## References

- [1] C. A. Angell, *Science* 267 (1995) 1924.
- [2] F. H. Stillinger, *Science* 267 (1995) 1935.
- [3] M. D. Ediger, C. A. Angell, S. R. Nagel, *J. Phys. Chem.* 100 (1996) 13200.
- [4] C. A. Angell, *J. Phys. Cond. Mat.* 12 (2000) 6463
- [5] M. D. Ediger, *Annu. Rev. Phys. Chem.* 51 (2000) 99.
- [6] N. Menon, S. R. Nagel, *Phys. Rev. Lett.* 73 (1994) 963.
- [7] A. van Blaaderen, P. Wiltzius, *Science* 270 (1995) 1177.
- [8] W. van Meegen, T. C. Mortensen, S. R. Williams, J. Müller, *Phys. Rev. E* 58 (1998) 6073.
- [9] W. Kob, J. L. Barrat, F. Sciortino, P. Tartaglia, *J. Phys. Cond. Mat.* 12 (2000) 6385.
- [10] P. N. Pusey, W. van Meegen, *Nature* 320 (1986) 340.
- [11] L. Cipelletti, S. Manley, R. C. Ball, D. A. Weitz, *Phys. Rev. Lett.* 84 (2000) 2275.
- [12] L. Cipelletti, H. Bissig, V. Trappe, P. Ballesta, S. Mazoyer, *J. Phys.: Condens. Matter* 15 (2003) S257.

- [13] R. E. Courtland, E. R. Weeks, *J. Phys.: Condens. Matter* 15 (2003) S359.
- [14] W. K. Kegel, A. van Blaaderen, *Science* 387 (2000) 290.
- [15] E. R. Weeks, J. C. Crocker, A. C. Levitt, A. Schofield, D. A. Weitz, *Science* 287 (2000) 627.
- [16] I. Snook, W. van Megen, P. N. Pusey, *Phys. Rev. A* 43 (1991) 6900.
- [17] W. G. Hoover, F. H. Ree, *J. Chem. Phys* 49 (1968) 3609.
- [18] D. R. Nelson, M. Widom, *Nucl. Phys. B* 240 (1984) 113.
- [19] D. R. Nelson, *Defects and Geometry in Condensed Matter Physics*, Cambridge University Press, 2002.
- [20] F. H. Stillinger, *J. Chem. Phys.* 89 (1988) 6461.
- [21] S. A. Kivelson, X. Zhao, D. Kivelson, T. M. Fischer, C. M. Knobler, *J. Chem. Phys.* 101 (1994) 2391.
- [22] A. D. Dinsmore, E. R. Weeks, V. Prasad, A. C. Levitt, D. A. Weitz, *App. Optics* 40 (2001) 4152.
- [23] L. Antl et. al., *Colloids and Surfaces* 17 (1986) 67.
- [24] J. C. Crocker, D. G. Grier, *J. Colloid Interface Sci.* 179 (1996) 298.
- [25] A. Kose, S. Hachisu, *J. Colloid Interface Sci.* 55 (1976) 487.
- [26] A. Gast, W. Russel, C. Hall, *J. Colloid Interface Sci.* 55 (1986) 161.
- [27] G. C. Cianci, R. E. Courtland, E. R. Weeks, to be published in the Proceedings for the 3rd Workshop on Complex Systems (cond-mat/0511301).
- [28] E. R. Weeks, D. A. Weitz, *Phys. Rev. Lett.* 89 (2002) 095704.
- [29] D. N. Perera, P. Harrowell, *J. Chem. Phys.* 111 (1999) 5441.
- [30] J. .C. Conrad, F. W. Starr, and D. A. Weitz, *J. Phys. Chem. B* 109 (2005) 21235.